Stacking faults in the structure of nickel hydroxide: a rationale of its high electrochemical activity

Claude Delmas* and Cecile Tessier

Institut de Chimie de la Matière Condensée de Bordeaux-CNRS and Ecole Nationale Supérieure de Chimie et Physique de Bordeaux, Av. Dr A. Schweitzer, Château de Brivazac, 33608 Pessac cédex, France

The usually observed broadening of some lines in the X-ray diffraction pattern of $Ni(OH)_2$ is shown to result from the presence of stacking faults leading to the existence of some fcc domains within the hexagonal compact oxygen packing. Simulation of the X-ray diffraction pattern with the DIFFaX program allowed us to propose a structural model and to estimate the amount of defects. The existence of these stacking faults explains in a very convenient way the relation between the line broadening and both the electrochemical behaviour and the presence of unexpected bands in the Raman spectra.

Nickel hydroxide is the positive electrode material of alkaline secondary batteries (Ni–Cd, Ni–MH [metal hydride], Ni–H_2). Depending on the preparation conditions, the crystallite size can vary in a wide range; nevertheless, most classical preparation conditions lead to small platelets (a few 100 Å in diameter and 100–300 Å in thickness) which exhibit good electrochemical activity. For years, numerous studies have been carried out in order to try to improve this activity through modification of the texture of the material.

Several years ago a very poorly crystallised nickel hydroxide denoted β_{bc} (badly crystallised) was reported in our laboratory.[1] This material, obtained by the ageing of α-nickel hydroxide, exhibits an X-ray diffraction pattern with very broad (001) and (10*l*) lines, while the (*hk*0) lines remain quite narrow. This feature is characteristic of a platelet like texture. Nevertheless, the presence of a large amount of sulfate ions (the SO_4^{2-}/Ni^{2+} ratio varies between 0.10 and 0.17) suggests that this material is an intermediate between the classical nickel hydroxide and a nickel hydroxysulfate. From this point of view, the structure can be considered as an interstratified one, in good agreement with the shape of the (001) line and the presence of both a narrow and a very broad band in the 4000–2500 cm^{-1} range in the IR spectra.[1]

Among the various studies devoted to the relation between the electrochemical activity and the crystallite size, those of Terasaka *et al.*[2] and Bernard *et al.*[3] must be mentioned. More recently, a systematic study of the electrochemical, physical and structural properties allowed Bernard and co-workers to clearly relate the electrochemical activity and the apparent abnormal broadening of the (10*l*) and (20*l*) diffraction lines to the existence of structural defects which lead to a new unexpected line on the Raman spectra.[4] These authors have hypothesised proton vacancies which could explain satisfactorily the Raman spectra. Moreover, as the same effect is observed when cobalt (Co^{3+}) is partially substituted for nickel, this hypothesis seems to be reinforced.

Nevertheless, one question remains: why is the X-ray diffraction pattern so strongly modified by the existence of a relatively small number of point defects? Fig. 1 gives as an example the X-ray diffraction patterns of several nickel hydroxides obtained from various synthesis conditions. From these patterns, determination of the crystallite size using the Scherrer formula leads to incoherent results. Indeed, from the broadening of the (001) and (100) lines, the thickness and the diameter of the particles (assuming a cylindrical shape) can be calculated. The problem arises from the considerably lower values of the coherence length along (10*l*) lines for example. Therefore, it seems that the number of planes which lead to constructive interferences

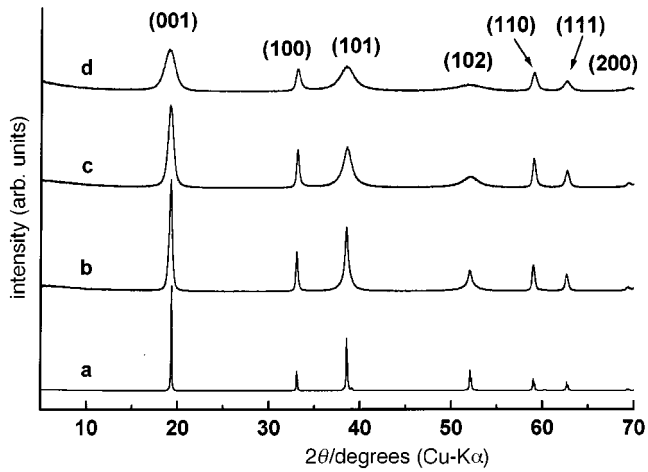

Fig. 1 X-Ray diffraction patterns of nickel hydroxide obtained under various conditions: (a,b) hydrothermal recrystallisation at 200 and 150 °C respectively; (c) precipitation at 70 °C, drying at 120 °C; (d) precipitation at 20 °C, drying at 60 °C

during the X-ray diffraction process varies with the plane orientation. In the wake of this remark, the existence of stacking faults within the structure can be hypothesised. Such a hypothesis was very recently proposed by Wronski *et al.* who compared the broadening of the nickel hydroxide X-ray diffraction pattern with that observed in some metals.[5] A point along these lines was made a long time ago by Barnard *et al.* who claimed that 'the selective line broadening is consistent with misalignment along the basal plane of a laminar structure'.[6] As the hypothesis of extended structural defects seems particularly convenient to explain the overall behaviour of nickel hydroxide, we have reconsidered its structure, not only by classical diffraction techniques, but also by simulating the effect of stacking faults on the shape of the X-ray diffraction patterns.

Only few structural studies of $Ni(OH)_2$ have been reported. One must consider the neutron diffraction experiments of Szytula *et al.*[7] and the more recent one of Greaves and Thomas[8] using the Rietveld refinement method. In both cases the structural determination has been carried out on materials obtained by hydrothermal syntheses, *i.e.* with large crystallite size suitable for structural characterisation. Both cases are in accord with the CdI_2 structure type and gave quite similar results. The structure will be further described in this paper. A study of a more classical hydroxide obtained by direct precipi-

tation was also undertaken by Greaves and Thomas[8] These authors mentioned the presence of new weak peaks on the neutron diffraction pattern, which were attributed to the existence of structural defects. Nevertheless, the poor quality of the neutron diffraction pattern prevented any precise structural determination.

This survey clearly shows that a new approach to the structure description is required in order to understand the behaviour of the real material used in batteries which is always poorly crystallised. This paper reports the first structure description under the hypothesis of the existence of stacking faults which lead to a theoretical diffraction pattern very similar to the experimental one.

Experimental

Nickel hydroxides were obtained by direct precipitation from 1 M $NiSO_4$ and 2 M NaOH solutions. In order to obtain homogeneous materials, the nickel solution is introduced into the NaOH solution; as an excess (50%) of NaOH is used, the pH remains equal to 14 during the whole precipitation process. The two hydroxides with best crystallinity were obtained by hydrothermal treatment (150 °C and 200 °C respectively) of the precipitated material.

X-Ray diffraction patterns were obtained with a Siemens D5000 diffractometer with a Cu-Kα radiation ($\lambda = 1.541\,78$ Å).

The DIFFaX program was used for the simulation of the X-ray diffraction patterns.[9] It consists of building the various types of slabs present within the material from the ideal atomic positions and the unit-cell parameters. Then, these slabs are packed along the *c* direction with a translational vector which possibly introduces the stacking faults. Simulations were made for a random distribution of faulted planes. Pseudo-Voigt functions were used to define the shape of the diffraction lines; the (100), (110) and (200) lines were used to determine the *u*, *v*, *w* pseudo-Voigt parameters because these lines are not affected by the presence of stacking faults (as will be discussed in the following).

In a first step, the effect of both the number and type of stacking faults on the shape of the X-ray patterns was considered in a very general manner; therefore, no contribution of the crystallite size on the line broadening was directly considered. In this case, an infinite number of slabs and the *u*, *v*, *w* parameters obtained from the X-ray diffraction pattern of well crystallised nickel hydroxide [Fig. 1(a)] were used.

In a second step, trials were made in order to simulate one experimental pattern as accurately as possible. In this case, the FWHM of the (001) line allowed us to define the crystallite thickness.

Results and Discussion

General overview of the structure and the stacking faults

The ideal structure of nickel hydroxide can be described from a packing of $Ni(OH)_2$ slabs. Since the oxygen packing is ABAB, one slab only is present within the unit cell, which is therefore hexagonal ($a = 3.132$ Å, $c = 4.611$ Å, space group $P\bar{3}m1$). The slabs are built up of edge-sharing NiO_6 octahedra; within the interslab space, the hydrogen atoms are located in tetrahedral environments exactly above or below the oxygen atoms. In this packing, if one considers the 'HO_4' tetrahedra, the third Pauling rule is obeyed since all polyhedra share only edges. This tendency to share polyhedra edges rather than corners explains why the $M(OH)_2$ hydroxides exhibit the ABAB packing, which allows a minimisation of electrostatic interactions for such material formula. Therefore, during the growth of the particles perpendicular to the slab, the new oxygen layer tends to be exactly superimposed on the last but one. A Rietveld refinement of the X-ray diffraction pattern of a very well crystallised material [Fig. 1(a)] allowed determination of the oxygen position (1/3, 2/3, 0.206), the nickel ion being in position (0, 0, 0). This oxygen position is in agreement with that reported in the literature.[7,8] These two positions which allow one to define the structure of an individual slab were used in all simulations.

Sebastian and Krishna have discussed in detail the effect of stacking faults in hexagonal compact (hc) and face centred cubic (fcc) packings.[10] From a general point of view, they consider three main types of stacking following a stacking fault: (i) in the 'growth fault', the structure continues to grow with its natural packing rule, (ii) in the 'deformation fault', a part of the structure is displaced and (iii) in the 'layer displacement fault', only one layer has been modified in the part of the crystal considered.

In the case of nickel hydroxide, the crystal formation cannot be considered as a layer by layer growth but as a slab by slab growth. Therefore, the various types of stacking faults must be considered in a more general manner since the two oxygen layers of an $Ni(OH)_2$ slab do not play the same role. Therefore, the first two types of defects lead to the formation of fcc blocks (ABC) within the normal ABABAB oxygen packing while the layer displacement fault leads simultaneously to the formation of fcc and non-close-packing (AA) blocks. At the present stage of our work only the first two models have been considered as relevant. Moreover, as the natural tendency of $Ni(OH)_2$ is to have an hc packing, it has been considered that after the defect, the growth continues with the hc packing. Therefore, the following two oxygen packings have been considered:

'growth faults'

ABABABC̲BCB…CBCBA̲BABAB …

'deformation faults'

ABABABC̲ACA … CACAB̲CBC … BCA̲BABABAB …

In these schemes, the faulted planes, which are randomly distributed, are underlined. In the first one, only one isolated fcc block (ABC) is present, while in the second packing type considered, two fcc blocks occur consecutively (ABC and BCA) in the ABCA sequence. Actually, as it will be discussed in the following, a mixture of the two types of defects is required to simulate the experimental patterns.

Effect of the presence of stacking faults on the X-ray diffraction patterns

The simulations were performed for the two structural models for an amount of stacking faults ranging between 0 and 20%. The general changes of the simulated X-ray diffraction patterns in growth and deformation fault hypotheses are shown in Fig. 2 and 3, respectively. In both figures the X-ray pattern simulated for the ideal structure, *i.e.* without stacking fault, is shown in (a). In the 2θ range considered, only the shape of the ($10l$) lines is modified. The simulation in the whole angular domain shows that only the ($h0l$) lines are broadened in good agreement with the theoretical calculation reported by Sebastian and Krishna.[10] A comparison of the shape modification when the amount of stacking faults increases emphasises very different effects. In the case of the deformation fault there is a tendency to a splitting of the (102) diffraction line, while in the case of the growth fault the centre of the line becomes very narrow, whereas the wings become rather broad. At first sight the shape modifications *vs.* the stacking fault amount seem less important for the growth fault than in the case of the deformation fault; therefore, only three patterns have been reported in Fig. 2. This difference in shape evolution is very interesting for the simulation of the experimental spectra as it allows consideration of the mixing of the two types of defects in a reasonable way.

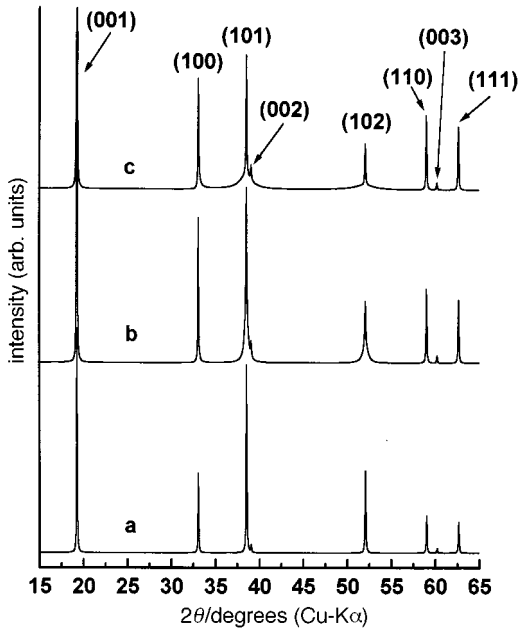

Fig. 2 Simulated X-ray diffraction patterns of nickel hydroxide in the hypothesis of growth stacking faults [(a) ideal structure; (b) 5%, (c) 20% stacking faults]

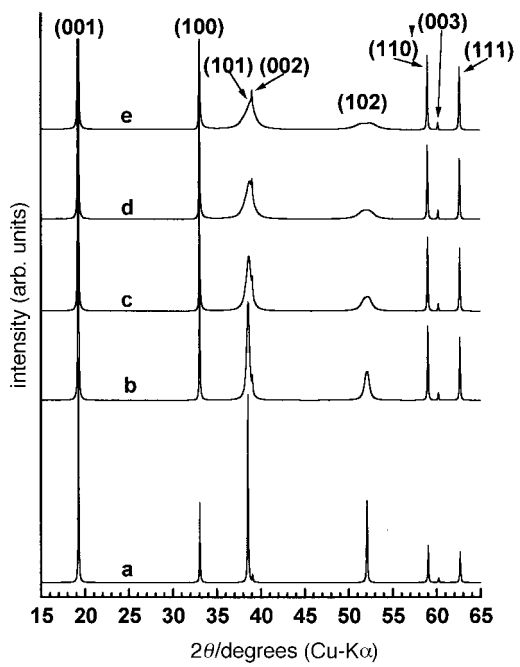

Fig. 3 Simulated X-ray diffraction patterns of nickel hydroxide in the hypothesis of deformation stacking faults [(a) ideal structure; (b) 5%, (c) 10%, (d) 15%, (e) 20% stacking faults]

Comparison with the experimental patterns

General comparison. The simulated pattern of the ideal material [Fig. 2(a) and 3(a)] is very close to the experimental one obtained for well crystallised nickel hydroxide [Fig. 1(a)] synthesised under strong hydrothermal conditions (200 °C). This result shows that the ideal structure is the most stable one and this not only leads to large particles but also eliminates the structural defects. The pattern obtained in the hypothesis of 5% of growth faults [Fig. 2(b)] looks like that of Fig. 1(b) for nickel hydroxide obtained by hydrothermal synthesis under soft conditions (150 °C). The patterns represented in Fig. 3(c)–(e), which have been obtained with the deformation fault hypothesis (10, 15, 20%) seem rather related to those of nickel hydroxides obtained directly by precipitation and drying [Fig. 1(c), (d)]. Nevertheless, as will be discussed in detail in the following, the agreement can be improved by considering the simultaneous presence of the two types of defects. In all cases, the broadening of (10*l*) lines increases when the amount of stacking faults increases. Moreover, the experimental patterns shown in Fig. 1 show an increase in the (001) linewidth when the synthesis temperature decreases, as a result of the decrease in particle size along the *c* direction. As the simulation has been realised for an infinite number of slabs, the difference between the width of the (001) line of experimental and simulated patterns increases when the particle size decreases.

Simulation of an experimental pattern. The experimental diffraction pattern given in Fig. 1(c) has been selected for the simulation. It corresponds to that of a classical nickel hydroxide used in alkaline batteries. In this simulation all structural and textural parameters (platelets thickness and diameter) have been considered. As discussed in the previous experimental section, the number of NiO_2 slabs along the *c* direction was calculated from the broadening of the (001) diffraction line using the Scherrer formula. In the material studied the average number of slabs is equal to 60. Then, from the shape of the (100), (110) and (200) diffraction lines which are not sensitive to the presence of stacking faults, the *u*, *v*, *w* parameters which characterise the pseudo-Voigt function have been determined with the Profile program.[11] These parameters are equal to 4.94, −4.20 and 0.91, respectively. Under these conditions, the broadening of the X-ray diffraction lines resulting from the particle size and from the experimental conditions of the X-ray diffraction experiment are automatically included in the simulation.

In a first step, a simulation of the X-ray diffraction pattern of a nickel hydroxide with the experimental particle size but with the ideal structure, *i.e.* without stacking faults, was done. This pattern is shown in Fig. 4(c). Comparison with the experimental one [Fig. 4(b)] shows, as expected, a good agreement for the (001), (100), (110) and (111) lines, while a very strong discrepancy is observed for the (101) and (102) lines.

In a second step, an increasing amount of stacking faults was introduced in the two previously described hypotheses. In

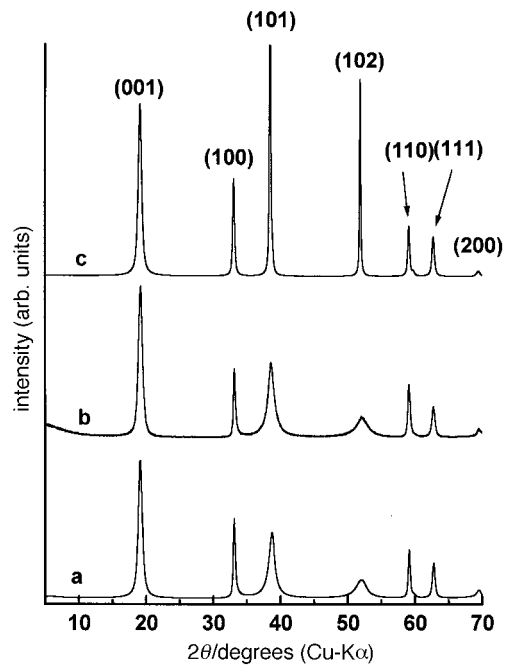

Fig. 4 Comparison of the experimental diffraction pattern of a nickel hydroxide (b) with simulated patterns without stacking faults (c), and in the hypothesis of the simultaneous presence of 10% of deformation faults and 8% of growth faults (a)

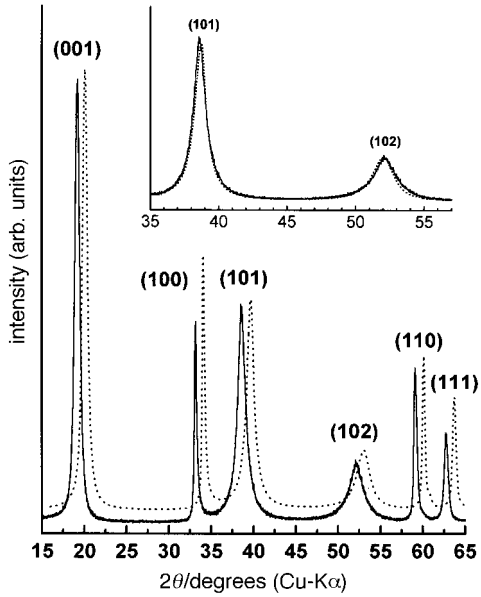

Fig. 5 Comparison of the experimental diffraction pattern of a nickel hydroxide (continuous line) with the simulated pattern in the hypothesis of the simultaneous presence of 10% of deformation faults and 8% of growth faults (dotted line). In the main figure, the simulated pattern has been shifted by one degree to the right.

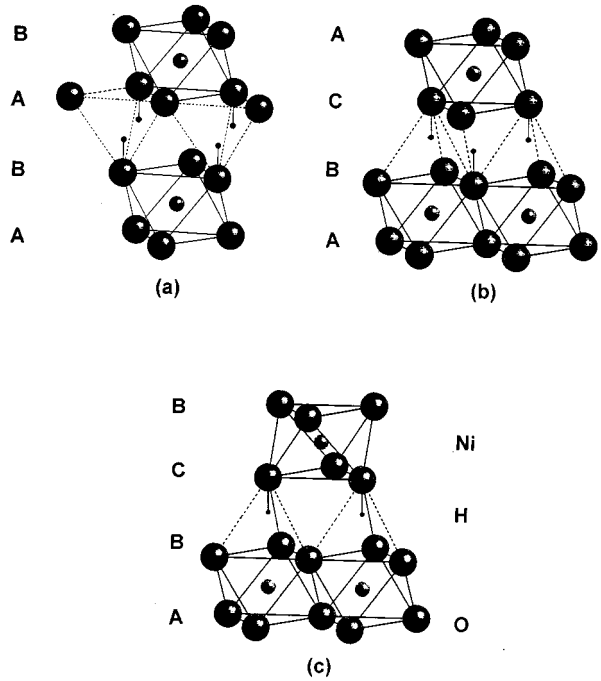

Fig. 6 Polyhedra linkages illustrating the interaction between the hydrogen atom of the hydroxide slab and one nickel ion of the next slab: (a) in the ideal structure (ABAB oxygen stacking), (b) on a deformation stacking fault (ABCA oxygen stacking) and (c) on a growth stacking fault (ABCB oxygen stacking)

both cases, a significant broadening of the (101) and (102) lines was observed but the shape of the lines did not fit satisfactorily. Then, from the best simulation obtained in the 'deformation fault' hypothesis an increasing amount of 'growth fault' was introduced. The best result was obtained for the simultaneous presence of 10% of 'deformation faults' and 8% of 'growth faults'. The resulting simulated X-ray diffraction pattern represented in Fig. 4(a) is quite similar to the experimental one. In order to clearly emphasise the similitude between the experimental and the simulated patterns, they are shown in an expanded scale in Fig. 5. The difference between the two patterns is so small that, in order to distinguish the simulated from the experimental one, the former pattern has been shifted by 1 degree to the right. Moreover, the (101) and (102) lines of the two patterns, which are very sensitive to the presence of stacking faults, are superimposed in the insert of the same figure. The very good agreement between the simulated and the experimental patterns confirms the presence of both types of stacking faults in nickel hydroxide.

Fig. 6 presents a comparison of a small part of the structure for the ideal material (ABAB packing) and in the vicinity of a stacking fault for the two hypotheses (ABCB and ABCA packings). While in the ideal structure the electrostatic interaction between a hydrogen atom and a nickel ion is quite small (the 'HO_4' tetrahedron and the NiO_6 octahedron share only one edge), in the vicinity of a stacking fault this interaction is much larger as the two polyhedra share one face, in violation of the third Pauling rule. It results that the hydrogen atoms localised at the stacking faults are destabilised with respect to the others. Thus, during the charge of the battery they can be more easily deintercalated. One can assume that at the following battery discharge, hydrogen atoms will not be easily reintercalated into these sites, leading to the persistence of trivalent nickel ions which may provide a local electronic conductivity and therefore improve the electrochemical activity. Moreover, the comparison of the environments for the two stacking faults shows that the number of face-sharing polyhedra for the deformation fault is twice that for a growth fault; therefore, the destabilisation is greater for the deformation fault than for the growth fault.

The presence of these hydrogen atoms in a different surrounding explains the appearance of new lines in the Raman spectra. The electrostatic Ni–H interactions which increase with the number of stacking faults lead to an increase of the interslab distance, in good agreement with the experimental results reported in Fig. 1 which indicate a shift of the (001) line as previously mentioned by Bernard *et al.*[4]

The *c* parameter deduced from the position of the (001) line is therefore an average value due to the existence of three types of interslab spaces: the ideal one and those corresponding to the growth and deformation faults. The presence of such a distribution of interslab spaces along the *c* axis shows that the true structure description is even more complicated than the model used for the simulation reported in the previous section. Such a distribution of interslab spaces can be considered as an interstratification phenomenon which is well known to broaden and displace the X-ray diffraction lines. At the present status of our simulations it is not reasonable to try to introduce new variable parameters since the interslab thicknesses are not known. Nevertheless, this small interstratification phenomenon can explain the slight difference in position of the (101) and (102) lines between the experimental and the simulated patterns shown in Fig. 5.

Conclusion

For the first time, a simulation of the X-ray pattern of nickel hydroxide has been realised with the hypothesis of the presence of stacking faults randomly distributed in the oxygen hexagonal compact packing. This simulation explains the abnormal broadening of some diffraction lines observed on the experimental pattern. In the vicinity of a stacking fault, the strong electrostatic interactions between the nickel ions and the hydrogen atoms lead to a destabilisation of the latter which improves the electrochemical activity. Numerous studies are necessary in order to describe these defects in a more precise way, as well as the effect of dopants like cobalt. This cation remains in the trivalent state in nickel hydroxide; therefore, proton vacancies are required to ensure the charge balance, so that one can expect a strong relation between the presence of cobalt and the occurrence of a large amount of stacking faults

leading to the high electrochemical activity of cobalt-doped nickel hydroxides. It is commonly mentioned in the literature that substitution of a small amount of cobalt for nickel improves the conductivity of the hydroxide. Whereas it is evident that the presence of protonic vacancies increases the ionic conductivity, the effect on electronic conductivity was not obvious as trivalent cobalt in the low-spin state is a diamagnetic ion. If one assumes that the presence of cobalt ions increases the number of stacking faults, as suggested by the X-ray diffraction patterns, the electronic conductivity on cycling of the cobalt-doped hydroxide will be improved, thanks to the induced stabilisation of trivalent nickel at the end of discharge.

The approach proposed in this paper may lead to a reconsideration of the overall electrochemical properties of the β-type nickel hydroxide.

The authors wish to thank J. Pannetier (Péchiney), P. H. Haumesser, C. Léger, J. P. Pérès, M. Ménétrier and L. Guerlou-Demourgues for fruitful discussions and SAFT and ANRT for financial support. CNES, DRET and Région Aquitaine are thanked for their contribution to the purchase of the Siemens diffractometer.

References

1 C. Faure, C. Delmas and M. Fouassier, *J. Power Sources*, 1991, **35**, 279.
2 M. Terasaka, M. Kanbayashi and T. Shiojidi, *Jpn. Pat*., 1991, 541213.
3 M. C. Bernard, P. Bernard, M. Keddam, S. Senyarich and H. Takenouti, *Electrochim. Acta*, 1996, **41**, 91.
4 M. C. Bernard, R. Cortes, M. Keddam, S. Senyarich, H. Takenouti and P. Bernard, *J. Power Sources*, in press.
5 Z. Wronski, G. Carpenter and P. Kalal, *190th Electrochem. Soc. Meet., Abstr*., 1996, p. 758.
6 R. Barnard, C. F. Randell and F. L. Tye, *Power Sources 8*, Academic Press, London, 1981, p. 401.
7 A. Szytula, A. Murasik and M. Balanda, *Phys. Status Solidi B*, 1971, **43**, 125.
8 C. Greaves and M. A. Thomas, *Acta Crystallogr., Sect. B*, 1986, **42**, 51.
9 M. Treacy, J. Newsam and M. Deem, *Proc. R. Soc. London Ser. A*, 1991, **43**, 499.
10 M. T. Sebastian and P. Krishna, *Random, Non-Random and Periodic Faulting in Crystals*, Gordon and Breach Science Publishers, London, 1994.
11 Diffrac-AT, V3-2, Siemens, Socabim, 1993.

Paper 7/01037K; *Received* 13*th February*, 1997